

ECOLOGY LETTERS

Predicting present and future intra-specific genetic structure through niche hindcasting across 24 millennia

Journal:	<i>Ecology Letters</i>
Manuscript ID:	ELE-01218-2011.R2
Manuscript Type:	Letters
Date Submitted by the Author:	n/a
Complete List of Authors:	Espíndola, Anahí; University of Lausanne, Department of Ecology and Evolution Pellissier, Loïc; University of Lausanne, Department of Ecology and Evolution Maiorano, Luigi; University of Lausanne, Department of Ecology and Evolution Hordijk, Wim; University of Lausanne, Department of Ecology and Evolution Guisan, Antoine; University of Lausanne, Department of Ecology and Evolution Alvarez, Nadir; University of Lausanne, Department of Ecology and Evolution
Key Words:	Hindcasting, species distribution models, phylogeography, past climate, <i>Trollius europaeus</i> , post-glacial contraction, recolonization, forecasting, climate change, AFLP



1 Title: Predicting present and future intra-specific genetic structure through niche hindcasting
2 across 24 millennia

3
4 Anahí Espíndola^{a*}, Loïc Pellissier^{a*}, Luigi Maiorano^a, Wim Hordijk^a, Antoine Guisan^{a†},
5 Nadir Alvarez^{a†}

6 *Anahí Espíndola and Loïc Pellissier equally contributed to this study and should be
7 considered as co-first authors.

8 †Nadir Alvarez supervised Anahí Espíndola and Antoine Guisan supervised Loïc Pellissier.

9
10 ^aDepartment of Ecology and Evolution, Biophore Building, University of Lausanne, 1015
11 Lausanne, Switzerland.

12 Author contributions: AE, LP and NA designed the study, AE and LP collected data, AE
13 performed the phylogenetic analyses, LP, LM and WH performed the modelling work, AE
14 and LP performed the meta-analysis, AE wrote the first draft of the manuscript, and all
15 authors contributed substantially to revisions.

16 Email addresses: Anahí Espíndola: anahi.espindola@gmail.com; Loïc Pellissier:
17 loic.pellissier@unil.ch; Luigi Maiorano: luigi.maiorano@unil.ch; Wim Hordijk:
18 wim@worldwidewanderings.net; Antoine Guisan: antoine.guisan@unil.ch; Nadir Alvarez:
19 nadir.alvarez@unil.ch

20 Running title: Hindcasting-based phylogeography

21 Type of article: Letter

22 Abstract: 150

23 Complete manuscript: 6786

24 Main text: 4700

25 Number of references: 50

26 Number of figures: 3

1
2
3
4
5
6
7
8
9
10
11
12
13
14
15
16
17
18
19
20
21
22
23
24
25
26
27
28
29
30
31
32
33
34
35
36
37
38
39
40
41
42
43
44
45
46
47
48
49
50
51
52
53
54
55
56
57
58
59
60

1
2
3
4
5
6
7
8
9
10
11
12
13
14
15
16
17
18
19
20
21
22
23
24
25
26
27
28
29
30
31

27 Number of tables: 1

28 Corresponding author: Anahí Espíndola, Department of Ecology and Evolution, University of
29 Lausanne. Biophore Building, 2015 Lausanne, Switzerland. Phone: +41 (0) 21 692 4278. Fax:
30 +41 (0)21 692 4265. Email: anahi.espindola@gmail.com.

For Review Only

1
2
3
4
5
6
7
8
9
10
11
12
13
14
15
16
17
18
19
20
21
22
23
24
25
26
27
28
29
30
31
32
33
34
35
36
37
38
39
40
41
42
43
44
45
46
47
48
49
50
51
52
53
54
55
56
57
58
59
60

32 **Abstract**

33 Paleoclimatic reconstructions coupled with species distribution models and identification of
34 extant spatial genetic structure have the potential to provide insights into the demographic
35 events that shape the distribution of intra-specific genetic variation across time. Using the
36 globeflower *Trollius europaeus* as a case-study, we combine (i) Amplified Fragment Length
37 Polymorphisms, (ii) suites of 1,000-year stepwise hindcasted species distributions and (iii) a
38 model of diffusion through time over the last 24,000 years, to trace the spatial dynamics that
39 most likely fits the species' current genetic structure. We show that the globeflower comprises
40 four gene pools in Europe, which, from the dry period preceding the Last Glacial Maximum,
41 dispersed while tracking the conditions fitting their climatic niche. Among these four pools,
42 two are predicted to experience drastic range retraction in the near future. Our
43 interdisciplinary approach, applicable to virtually any taxon, is an advance in inferring how
44 climate change impacts species' genetic structures.

46 **Keywords**

47 AFLP, climate change, forecasting, hindcasting, past climate, phylogeography, post-glacial
48 contraction, recolonization, species distribution models, *Trollius europaeus*

1
2
3
4
5
6
7
8
9
10
11
12
13
14
15
16
17
18
19
20
21
22
23
24
25
26
27
28
29
30
31
32
33
34
35
36
37
38
39
40
41
42
43
44
45
46
47
48
49
50
51
52
53
54
55
56
57
58
59
60

50 Introduction

51 Current distributions are predominantly the result of the interaction between species'
52 environmental requirements (the niche *sensu* Hutchinson) and geographic variation of key
53 environmental factors (the realized environment; Guisan & Thuiller 2005), among which
54 climate plays a predominant role (Araújo & Pearson 2005). In the context of Quaternary
55 climatic oscillations, the ebb and flow of glacial dynamics caused dramatic species range
56 expansions and retractions, involving local extinction, migration, drift and adaptation (Hewitt
57 1999). The genetic structure of species is thus intimately related to spatial and temporal
58 variation in their distribution ranges, which in turn shapes the pattern and frequency of inter-
59 population genetic exchanges.

60 Changes in climate have often fragmented or reconnected populations of the same species,
61 with gene flow among populations being accordingly restricted or enhanced (Hewitt 1999).

62 As a result, the genetic variation within species has been structured spatially in distinct and
63 variably isolated gene pools. Identifying and explaining these genetic structures has been the
64 aim of phylogeography over the last twenty years (Avice 2009) and has gained new attention
65 due to the possible implications for forecasting the distribution of gene pools under climate
66 change (Etterson & Shaw 2001; Davis *et al.* 2005). Phylogeographic patterns in Europe have
67 been summarized into a few paradigms for temperate organisms, such as the ones represented
68 by the European beech *Fagus sylvatica*, the hedgehog *Erinaceus europaeus* and the brown
69 bear *Ursus arctos* (e.g., Hewitt 1999), showing genetically diverse gene pools that survived
70 cold periods in Southern peninsulas.

71 In contrast, cold-adapted species have only recently received attention compared to temperate
72 species and knowledge of their phylogeographic patterns has not yet been summarized into
73 major paradigms (e.g., Weider & Hobaek 2000; Abbott & Brochmann 2003; Brochmann *et*
74 *al.* 2003; Ehrich *et al.* 2007). While phylogeographic investigations of temperate organisms
75 provide information on the genetic consequences of postglacial expansion processes, the

1 76 study of cold-adapted species that are currently found fragmentarily distributed and under
2
3 77 refugial conditions in most of their range (*e.g.* at high altitudes) unravels the genetic
4
5 78 consequences of distributional contractions related to climate warming.
6
7
8 79 Species distribution models (SDMs) rely on the analysis of the climatic conditions shaping
9
10 80 the distribution of species (Guisan & Thuiller 2005). In the last decade, a few studies (Hugall
11
12 81 *et al.* 2002; Alsos *et al.* 2009; Freedman *et al.* 2010; Vega *et al.* 2010; Beatty & Provan 2011)
13
14 82 have used hindcasted SDMs in combination with phylogeographic surveys to detect past
15
16 83 spatial discontinuities in species distributions, and thus to identify possible past barriers to
17
18 84 gene flow. However, very few points in time were considered in studies so far – the present,
19
20 85 the Last Glacial Maximum (LGM) and sometimes an additional mid-point between these two
21
22 86 – providing limited information on past range changes, and therefore neglecting the
23
24 87 quantitative identification of detailed spatial dynamics. Circumventing this limitation has
25
26 88 been roughly achieved, for instance by assuming a linear change in temperature and
27
28 89 precipitations from 9 to 18 kya (Graham *et al.* 2010). Consequently, the lack of accurate
29
30 90 climatic estimates at several time periods between the present and the LGM precluded a
31
32 91 thorough interpretation of range-shifts through time. Hindcasting the distribution of species
33
34 92 based on a larger number of more continuous time steps (Maiorano *et al.* in press) and
35
36 93 combining these with modeled diffusion rules represent an advance to decipher a species'
37
38 94 spatial and genetic histories.
39
40
41 95 Here, we use climatic reconstructions for the past from a global circulation model to predict
42
43 96 short-time stepwise species potential distributions, going back to the LGM and further into the
44
45 97 past across the last 24 millennia, and show how this information can be integrated with large
46
47 98 phylogeographic surveys and with a spatial model of expansion/contraction filtered by habitat
48
49 99 suitability (hereafter referred to as diffusion model) to understand a species' spatio-temporal
50
51 100 history. This approach provides key data on the putative location of the past distribution of
52
53 101 gene pools and on the pathways that they followed during range expansions and contractions
54
55
56
57
58
59
60

1
2 102 across the last millennia. We illustrate the approach by investigating the past distributional
3
4 103 dynamics of the cold-adapted globeflower, *Trollius europaeus* L. (Ranunculaceae), by using
5
6 104 simulations to infer how past range-variation influenced its current intra-specific genetic
7
8 105 structure, and finally identifying how it will be affected in the future. This species is a well-
9
10 106 suited case-study because i) it is associated with cold and moist habitats that experienced
11
12 107 drastic spatial reshuffling in the last millennia (Hewitt 1996), and ii) a preliminary
13
14 108 phylogeographic survey of the species suggested several spatially structured gene pools
15
16
17 109 (Després *et al.* 2002).

18
19 110 Based on the historical and ecological knowledge of the species, we expect the combined use
20
21 111 of phylogeography and spatial modeling to provide detailed information on how the current
22
23 112 gene pools moved in space and time to reach their present range, and how they could evolve
24
25 113 in a warming future. More precisely, we predict that: i) the past range of the current gene
26
27 114 pools (retrieved from phylogeographic analyses) should be identified by hindcasting
28
29 115 approaches, ii) the most likely pathways followed by the different gene pools should be
30
31 116 recognizable using a spatio-temporal niche-based diffusion model, and iii) future genetic
32
33 117 structure can be forecasted based on the combination of allele distribution interpolation and
34
35 118 range predictions.

36
37
38
39 119

40 41 120 **Material and methods**

42 43 121 *Genetic data and analyses of the spatial genetic structure of T. europaeus*

44
45 122 Samples of *T. europaeus* were collected during the springs and summers of 2006-2008 at 79
46
47 123 locations throughout the European range of the plant (Fig. 1A, see Table S1 in Supporting
48
49 124 Information). An amplified fragment length polymorphism (AFLP; Vos *et al.* 1995)
50
51 125 procedure was done with *EcoRI* and *MseI* endonucleases. Digested fragments were selected
52
53 126 with two primer pairs and genotyped (see Appendix S1 in Supporting Information).
54
55
56
57
58
59
60

1 127 The genetic structure of the dataset was identified with ten Markov chain Monte-Carlo runs of
2
3 128 1,000,000 generations with a 200,000 burn-in period for an *a priori* number of gene pools K ,
4
5
6 129 ranging from 1 to 20 (200 runs in total) as implemented in STRUCTURE 2.2 (Falush *et al.*
7
8 130 2007). The most probable K was identified following Pritchard *et al.* (2000). In order to
9
10 131 confirm the genetic structure, a non-model-based approach was applied using the K-means
11
12 132 clustering technique as introduced by Hartigan & Wong (1979). Following Burnier *et al.*
13
14 133 (2009), we identified the number of clusters (K) that optimizes the inertia of the dataset. The
15
16 134 calculations were repeated 10,000 times starting at different random points, and were run in
17
18 135 the R 9.2.1 CRAN environment (R Core Development Group, 2009) using custom R scripts.
19
20 136 Finally, we performed Principal Coordinates Analyses (PCoA) using custom R-scripts, and an
21
22 137 AMOVA using GenAlex 6.3 (Peakall & Smouse 2006).
23
24
25
26
27

138

139 *Climatic data*

30 140 The current climatic data (averaged from 1950 to 2000) was obtained from the Climatic
31
32 141 Research Unit (Mitchell *et al.* 2004). Simulations of past climate were obtained from a
33
34 142 general circulation model based on the Hadley Centre climate model (HAD3; Singarayer &
35
36 143 Valdes 2010), and used to produce paleo-temperature and precipitation maps at a 15 km
37
38 144 spatial resolution over Europe (see Appendix S1). Simulations of future climate were based
39
40 145 on three general circulation models (HAD3, CSRIO2 and CGCM2) and four future emission
41
42 146 scenarios (a1, a1FI, b1, b2; 12 projections in total) from the Intergovernmental Panel on
43
44 147 Climate Change (IPCC 2001) averaged from 2070 to 2100.
45
46
47
48
49

148

149 *Species distribution modeling*

52 150 To model the distribution of the species we combined the available occurrences with a set of
53
54 151 six bioclimatic variables assumed to be important for alpine plants (Körner 2003): total
55
56 152 annual precipitation, summer precipitation, winter precipitation, annual mean temperature,
57
58
59
60

1
2 153 and mean warmest and coldest temperatures. Occurrences of *T. europaeus* with a spatial
3
4 154 accuracy of $\leq 15\text{km}$ were obtained from published databases and fieldwork (see Appendix
5
6 155 S1). This scale was chosen because of its wide application in most biodiversity databases
7
8 156 (*e.g.*, GBIF, www.gbif.org) and because it corresponded to the grid-size of all climatic grids.
9
10 157 Pseudo-absences were generated by selecting 10,000 random points across Europe and
11
12 158 weighted in the following analyses to ensure a balance between the prevalence of presences
13
14 159 and pseudo-absences. Based on Engler *et al.* (2011), the realized climatic niche was modelled
15
16 160 using five modeling techniques (Thuiller *et al.* 2009). We evaluated the predictive
17
18 161 performance of each model using a repeated split sampling approach with 50 repetitions,
19
20 162 using the Area Under the Receiver Operating Characteristic (ROC) Curve (AUC; Fielding &
21
22 163 Bell 1997) as evaluation metric. Following Marmion *et al.* (2009), we calculated for each
23
24 164 projection an average of the five modeling techniques weighted by their predictive power (see
25
26 165 Appendix S1 and Table S2 in Supplementary Information). The SDM was projected into the
27
28 166 past and into the future. We evaluated the accuracy of past range predictions by comparing
29
30 167 the hindcasted distribution and the unambiguous fossil record for the plant species (European
31
32 168 Pollen Database; <http://pollen.cerege.fr/fpd-epd/>).

33
34
35
36
37
38
39 16940 170 *Distributional dynamics simulation and best-fit scenario identification*

41 171 We transformed the probability maps obtained from the SDM projections into binary
42
43 172 presence/absence maps using the ROC plot method that maximizes both sensitivity and
44
45 173 specificity (Liu *et al.* 2005) and considered as unsuitable those regions known to have been
46
47 174 covered by ice during each time period (Ehlers & Gibbard 2004; Gyllencreutz *et al.* 2007).

48
49 175 We used simulations to identify the past dynamics of the four currently identified gene pools
50
51 176 (see Results section). We first randomly chose four suitable pixels to delimitate the original
52
53 177 regions occupied by the four gene pools at the cold period previous to the LGM (24,000 years
54
55 178 ago, 24 kya). The remaining suitable pixels were then assigned to one of these clusters using a
56
57
58
59
60

1
2 179 simple proximity rule (*i.e.*, suitable pixels were assigned to a given cluster as a function of
3
4 180 their linear distance to the closest starting pixel). This way, the position of the four starting
5
6 181 pixels defined the initial distribution of each genetic cluster. Then, for each following time-
7
8 182 step (every 1,000 years) and up to the present, any suitable pixel in a timeframe t could be
9
10 183 colonized by the genetic group from the closest suitable pixel from timeframe $t-1$, a procedure
11
12 184 that we refer to as diffusion.

13
14 185 Finally, we compared the fit of the current genetic structure predicted by the simulated
15
16 186 scenarios with the empirical population genetic assignments. For this, the majority rule
17
18 187 criterion was applied, assigning each genetically analyzed population to a cluster by
19
20 188 considering the highest assignment probability obtained when applying genetic clustering
21
22 189 approaches (*e.g.*, with STRUCTURE). A population was assumed to be properly recovered by
23
24 190 the model if it was assigned to the same genetic cluster both at the end of the simulation
25
26 191 process and with the direct molecular approach. The scenario harboring the highest proportion
27
28 192 of recovered populations was considered as the one having most properly recovered the
29
30 193 overall current genetic structure. We ran the simulations 10,000 times, providing a sufficient
31
32 194 number of possible scenarios to properly examine the most suitable hypotheses. For improved
33
34 195 computation speed, we implemented this function, written in C language, in the *MigClim* R
35
36 196 package.

37
38 197 Results from the assignments were also evaluated using the assignment test implemented in
39
40 198 AFLPOP 1.1 (Duchesne & Bernatchez 2002). Considering the best-fit simulated scenario,
41
42 199 four groups were defined *a priori* to further evaluate the samples assignment likelihoods. We
43
44 200 used default parameters, with a likelihood threshold sensitivity set to 0.1. In order to compare
45
46 201 this output with a standard genetic clustering (*i.e.*, STRUCTURE), we performed the same
47
48 202 analysis defining groups based on that spatial genetic structure evaluation.
49
50
51
52
53
54

55 203

56
57 204 *Insights into future genetic diversity*
58
59
60

1
2
3
4
5
6
7
8
9
10
11
12
13
14
15
16
17
18
19
20
21
22
23
24
25
26
27
28
29
30
31
32
33
34
35
36
37
38
39
40
41
42
43
44
45
46
47
48
49
50
51
52
53
54
55
56
57
58
59
60

205 We used the population-based observed values of presences and absences of alleles for the
206 whole studied area and interpolated their distribution using a raster IDW (Inverse Distance
207 Weighted) approach (cell size: 15km) in ArcGIS 9.3 (Environmental Systems Research
208 Institute, Redlands, CA). Levels of polymorphism were estimated by combining interpolation
209 of both presences and absences: i) a locus was considered as present, if the allele was at least
210 present once in a population (identification of monomorphic absences); ii) a locus was
211 considered as absent, if the allele was absent at least once in a population (identification of
212 monomorphic presences). Afterwards, all cells falling within the suitable areas predicted by
213 the different future scenarios were selected and, for each locus, we considered as polymorphic
214 all pixels presenting values of presences and absences ranging between 0.4 and 0.6. Future
215 levels of genetic diversity were calculated by averaging the proportion of polymorphic alleles
216 per cell. Eventual genetic losses were identified by comparing these predicted values with
217 those obtained for current conditions, based on the same interpolated dataset applied to the
218 current projection. We finally identified the regions predicted to be occupied by each gene
219 pool, by assigning each pixel to one gene pool, considering the same rule as for the
220 assignments in the past (see above). We then compared surface occupancy (in numbers of
221 pixels) of each gene pool, under current and future climatic conditions, for both the whole
222 Europe and each geographic region.

223

224 **Results**

225 *Spatial genetic structure of the globeflower*

226 All clustering methods used to analyze the 374 AFLP fragments amplified in 349 samples
227 consistently identified four gene pools (Fig. 1A; see Figures S1 and Appendix S1). These
228 gene pools were geographically structured and presented several suture zones (Fig. 1A) and
229 appeared to be well-segregated in the PCoA (see Figure S2 in Supporting Information). The
230 AMOVA indicated that 4% of the genetic variance was significantly explained by the four

1 231 gene pools (5.5% explained by variance between populations; 90.5% explained by variance at
2
3
4 232 the intra-population level; see Figure S2). Our results demonstrated (i) the presence of a
5
6 233 cluster specific to South-Eastern Europe, (ii) the admixed genetic identity of several locations
7
8 234 in the Southern Alps and Eastern Pyrenees, and (iii) the existence of an exclusive and
9
10 235 independent Northern Scandinavian cluster, different from the one found in Southern
11
12 236 Scandinavia, the Carpathians and Northern Poland.

13
14
15 237

16
17 238 *Past range dynamics and spatial diffusion of the gene pools*

18
19 239 The ensembled SDM properly recovered the current range of the globeflower (Fig. 1B).
20
21 240 Projected distributions suggest that, at the earliest time analyzed (*i.e.*, 24 kya), *T. europaeus*
22
23 241 was more widespread than today (see Figure S3 in Supporting Information). At that time, the
24
25 242 distribution also appeared to be somewhat fragmented, with four centers of high climatic
26
27 243 suitability observed in the current Balkans, North-Eastern and North-Western Europe and the
28
29 244 Baltic zone. Past projections showed that hindcasted regions included the known fossil
30
31 245 records (see Figure S4 in Supporting Information), confirming the accuracy of the model. The
32
33 246 10,000 simulated scenarios provided varying outcomes and fits to the observed data (Fig. 2A;
34
35 247 see Figure S5 in Supporting Information). The two best scenarios properly assigned 83.5% of
36
37 248 the current spatial genetic structure. Because they were largely similar, only one of the two is
38
39 249 discussed (Fig. 2B; also see Figure S4). The best 5% of the simulations recovered trends
40
41 250 similar to these two best scenarios, assigning the sources of colonization of each of the four
42
43 251 clusters to the Pyrenees-Massif Central, to North-Western Europe, to the Balkans and to
44
45 252 North-Eastern Europe (Fig. 2B; see Figure S4 in Supporting Information). The best scenarios
46
47 253 of the range dynamics (Fig. 2B) indicated that the range of the plant largely increased with the
48
49 254 onset of the period generally associated to the LGM (21-18 kya), and strongly contracted at
50
51 255 around 12 kya, to finally reach its current range (see Figures S4 and S6 in Supporting
52
53 256 Information).

1
2 257 The assignment analysis performed using AFLPOP and the simulation outputs as a grouping
3
4 258 factor recovered similar assignment fits than our simulations, with 17.6% of samples being
5
6 259 assigned to other genetic clusters (versus 6.7% using the STRUCTURE clusters).
7
8
9

260

261 *Future distribution*

262 Range predictions for the next 60 years, under three climatic models and four emission
263 scenarios, showed that the distribution of the globeflower will be strongly modified in the
264 future (Fig. 3 and see Figure S6). The species distribution is predicted to shift to higher
265 elevations and latitudes, leading in some cases (*e.g.*, scenario CGCM-a2) to a final increase in
266 the total occupied area (Table 1), following a wide colonization of Scandinavia, and despite
267 extinctions in Southern European regions. Such extinctions are expected to strongly reduce
268 the ranges of two of the four gene pools (red and blue; Table 1 and Fig. 3), which are
269 predicted to respectively survive at the Western and Eastern edges of the Alps under some
270 scenarios only (see Figure S6). Moreover, based on interpolations of allele polymorphism in
271 future suitable areas, while some scenarios predict almost invariable diversity values
272 compared to current conditions, others forecast losses of up to 28% of the genetic diversities
273 (Table 1). Under the CSIRO2 circulation model, the percentage of genetic diversity loss
274 appeared to be linked to the strong decrease in the occupied surface. In all cases, Scandinavia
275 is predicted to harbor the most diverse areas, causing, under some scenarios, an overall
276 increase in the genetic diversity of *T. europaeus* (Table 1, Fig. 3). Scandinavia is also
277 expected to harbor more than 80% of the future surface occupancy (against 67% nowadays),
278 whatever climatic scenario is considered (see Figure S6).

279

280 **Discussion**

281 The interdisciplinary approach proposed in this study allowed modeling the changes that
282 affected the distribution of *T. europaeus* over the course of the last 24 millennia and that

1 283 shaped its current genetic structure. We demonstrated here that, in the case of *T. europaeus*,
2
3
4 284 the main trends in the range dynamics of its gene pools across the last millennia can be
5
6 285 reconstructed using spatial simulations closely matching empirical data (83.5%). Our
7
8 286 hindcasting-based approach therefore supports the use of niche-based SDMs to predict the
9
10 287 fate of species and gene pools in changing climatic conditions. We finally showed that
11
12 288 projecting our approach into the future allows predicting the expected variation in the total
13
14 289 range covered by each gene pool, determining which of them would be the most threatened
15
16 290 according to climate warming scenarios. These results also identified a variable loss of
17
18 291 diversity when associating SDMs to interpolated levels of polymorphism. In the next sections,
19
20 292 we discuss these findings in more detail as a way to illustrate the phylo- and biogeographic
21
22 293 information one can additionally gather with this approach.
23
24
25
26
27

294

28 295 *As many past centers of distribution as phylogenetic pools*

29
30 296 The total hindcasted range at 24 kya was in general congruent with the LGM hindcasted
31
32 297 distributions of other cold-adapted species from the region (see Figure S3; e.g., Svenning *et*
33
34 298 *al.* 2008) and indicated the presence of four centers of high habitat suitability. Based on more
35
36 299 samples and loci, a wider and more regular spatial covering and new analyses, the spatial
37
38 300 genetic structure identified in our results provides more informative insights into the
39
40 301 phylogeographic pattern of the European globeflower, when compared to a previously more
41
42 302 restricted study of this species (Després *et al.* 2002). We clearly identified the presence of
43
44 303 four gene pools (versus three supported groups in Després *et al.*, 2002), spatially structured
45
46 304 (Fig. 1A; see Figure S2) and restricted to South-Eastern (in blue, Fig. 1A), South-Western (in
47
48 305 red), North-Western and Central (in yellow), and North-Eastern Europe (in green).

49
50
51
52 306 The best-fit scenarios identified the Pyrenees-Massif Central, North-Western Europe, the
53
54 307 Balkans and North-Eastern Europe as the most likely sources of colonization of the current
55
56 308 range (Fig. 2B; see Figure S4), which largely corresponds to the distribution of suitability
57
58
59
60

1
2 309 values for *T. europaeus* populations at 24 kya, during the cold period preceding the LGM in
3
4 310 Europe (see Figure S3). This phase corresponded to a cold maximum, which, in Europe, was
5
6 311 associated with an arid period (Watts *et al.* 1996) that might have been too dry for the
7
8 312 globeflower to widely colonize the region.

9
10 313 It is worth noting that, besides identifying the most likely past sources of colonisation, our
11
12 314 procedure allowed for the recognition of a genetic relationship between regions spatially close
13
14 315 but separated in the past by a narrow unsuitable zone, such as the region laying between the
15
16 316 Pyrenees and the Massif Central (see Figure S3).

17
18
19
20 317

21
22 318 *Niche-based diffusion modeling helps identify the most likely phylogeographic dynamics*

23
24 319 The diffusion model allowed identifying two best-fit scenarios that correctly assigned 83.5%
25
26 320 of the genetically analyzed locations and, therefore, accurately tracking the paths followed by
27
28 321 the globeflower's gene pools across the last millennia. The two scenarios concurred in
29
30 322 showing that the climatic variations characterizing the last 24 ky largely drove the range
31
32 323 contractions and expansions experienced by *T. europaeus* (Fig. 2B; see Figures S4 and S6).

33
34 324 While the species had a relatively restricted range at 24 kya, its distribution showed an
35
36 325 expansion between 20-16 kya, probably related to the decrease in aridity in Europe (Watts *et*
37
38 326 *al.* 1996). After the beginning of the LGM, the species remained widespread for several
39
40 327 thousand years, with contact zones appearing between the gene pools. The establishment of a
41
42 328 long lasting warming period at around 15 kya caused the start of a strong contraction in the
43
44 329 species range. From then on, the gene pools moved to higher latitudes, and, in the Southern
45
46 330 European mountain ranges, to higher elevations. The cold Dryas period induced a modest
47
48 331 range expansion around 12 kya as the aridity did not increase (Watts *et al.* 1996), which likely
49
50 332 favored the spread of *T. europaeus*. After the end of this cold phase, the general tendency
51
52 333 towards a climate warming became established (Raymo 1997; Labeyrie *et al.* 2003). This
53
54 334 warmer period induced the final deglaciation of Northern Europe and of the Southern
55
56
57
58
59
60

1 335 mountain ranges, allowing a progressive colonization of regions previously covered by ice,
2
3 336 such as Scandinavia and the British Islands. As the climate began to warm, the West-
4
5
6 337 European and North-Eastern clusters, which reached Scandinavia between 10-5 kya,
7
8 338 continuously expanded their ranges until a contact zone arose in Northern Scandinavia. In
9
10 339 contrast, Southern gene pools of the species (i.e., South-Eastern and South-Western) remained
11
12 340 restricted to central and Southern European massifs and suffered a progressive range
13
14 341 reduction (Hewitt 1999).

15
16
17 342 Besides allowing for the identification of the most likely phylogeographic scenarios (Fig. 2),
18
19 343 our results explain the origin of contact zones. These were identified in the Alpine range, in
20
21 344 the Sudetes, in central Scandinavia and in Northern Scotland (Fig. 1A). While the first three
22
23 345 regions correspond to contact zones between neighbouring genetic lineages (yellow, blue and
24
25 346 red clusters in the Alps; yellow and blue clusters in the Sudetes; green and yellow clusters in
26
27 347 central Scandinavia; Fig. 1A), the fourth represents a more unexpected case of admixture that
28
29 348 may be explained by natural or anthropogenic long-distance dispersal. The Alpine contact
30
31 349 zone might be both a consequence of the ancient presence of the lineages in the region
32
33 350 (particularly for the Southernmost Italian population; Fig. 1A and 2B) and the centripetal
34
35 351 progressive colonization of higher elevations, related to the temperature increase of the last
36
37 352 thousand years (Fig. 2B). The best phylogeographic scenarios (Fig. 2B) help explaining the
38
39 353 contact zone in the Sudetes (Fig. 1A) suggesting the presence of the two gene pools in the
40
41 354 region during the LGM. They also allow explaining the formation of the Scandinavian contact
42
43 355 zone. Indeed, this region was unavailable (*i.e.*, under ice-sheets) or only locally available
44
45 356 (Parducci *et al.* 2012) during the coldest glacial phases, and appears to have been largely
46
47 357 colonized during the climate warming that happened between 10-5 kya. Our results are thus a
48
49 358 new evidence in plants (contrasting with results obtained in Schönswetter *et al.* 2006; Skrede
50
51 359 *et al.* 2006; Schmitt 2009; and in agreement with Parducci *et al.* 2012) that Scandinavia was
52
53 360 colonized by two distinct lineages that established a contact zone at mid latitudes. It is
54
55
56
57
58
59
60

1
2 361 however important to note that, in contrast to Parducci *et al.*, (2012), we do not find any
3
4 362 genetic signature (*e.g.*, presence of private alleles) suggesting a survival of *T. europaeus* in
5
6 363 Scandinavian glacial refugia.
7

8 364

9
10 365 *Incongruence between empirical and modeled spatial genetic structures*

11
12 366 The comparison of simulation- and genetic-based assignments showed some incongruence
13
14 367 (Fig. 2B), most likely corresponding to i) incorrect assignment of populations in contact
15
16 368 zones, and ii) long-distance dispersal events. Overall, however, incongruent assignments
17
18 369 accounted for less than one sixth of all populations, attesting the relevance of the approach
19
20 370 used here. The largest incongruence occurred at the Scandinavian contact zone, which was
21
22 371 shifted to the North in our simulations. This may be due to the fact that in our simulations
23
24 372 South-Western Scandinavia became suitable for the species before the Northern Scandinavian
25
26 373 edge was free of ice. Furthermore, the projection of our SDM at 24-10 kya indicated that
27
28 374 conditions in Northern Scandinavia were not suitable for *T. europaeus*, probably because of
29
30 375 the extreme drought associated to the proximity of ice-sheets. However, recent genetic and
31
32 376 paleoecological studies demonstrated that some areas at high latitudes were locally ice-free
33
34 377 during the last glaciations, providing putative shelter to cold-adapted species (Westergaard *et*
35
36 378 *al.* 2011; Parducci *et al.* 2012) and suggesting that an early local colonization of the North-
37
38 379 Western Scandinavian coasts by the North-Eastern gene pool could have been possible.
39
40 380 However, local ice-cover anomalies are not yet taken into account in the Eurasian ice-sheet
41
42 381 reconstructions available for the area and thus could not be considered in our simulations.
43
44 382 Alternative scenarios would be that the region was colonized through a long-distance
45
46 383 dispersal event (not considered in our model), and/or that more recent and quick demographic
47
48 384 dynamics have shuffled the precise location of this contact zone. In order to further
49
50 385 investigate these points, once more detailed and updated paleogeographical and
51
52
53
54
55
56
57
58
59
60

1
2 386 paleoglaceological maps become available, we recommend their implementation in
3
4 387 simulations modeling diffusion of gene pools.

5
6 388

7
8 389 *Predicting species range-shifts and genetic losses in response to climate warming*

9
10 390 When forecasting the range of the species for the next 60 years, our results indicated that

11
12 391 global warming is expected to negatively affect the range of the globeflower under some

13
14 392 scenarios only (Table 1), differentially influencing each gene pool (Fig. 3; see below and

15
16 393 Figure S6), and sometimes leading to a strong decrease of the European genetic diversity of

17
18 394 the species (Table 1). In contrast to temperate species, cold-adapted species mainly show

19
20 395 contracted refugial distributions during interglacial periods, such as the ongoing one (Stewart

21
22 396 *et al.* 2010). Under the climatic warming scenarios considered here, the range of the plant is

23
24 397 predicted to be more restricted to high elevations and latitudes than today, with the species

25
26 398 going almost extinct in most Southern mountain ranges (Fig. 3 and see Figure S6). The Alps

27
28 399 represent the most important future South-European refugia, presenting the largest suitable

29
30 400 area in the region and confirming an idea previously suggested by Alsos *et al.* (2009). Our

31
32 401 predictions additionally indicate that central Scandinavia will likely harbour the largest

33
34 402 genetic diversity in Europe (Fig. 3). Most future scenarios predict that a large part of the

35
36 403 genetic diversity will be lost in the Southern mountain ranges, and only a few scenarios

37
38 404 predict fair genetic diversity preservation in the Eastern Alps and the Sudetes (see Figure S6).

39
40 405 Our genetic diversity inferences for the future are somewhat similar (no loss, or losses of <

41
42 406 30%) to a recent predictive analysis done on a set of arctic-alpine plants (Alsos *et al.* 2012).

43
44 407 Indeed, the lack of genetic loss in some future scenarios (*e.g.*, CGCM2) is a result of the final

45
46 408 surface gain, which is particularly high in the diverse central Scandinavia (Fig. 3 D–H).

47
48 409 Genetic diversity values fall only when the range becomes patchy in the whole region, what

49
50 410 was observed under all emission scenarios applied to the CSIRO2 circulation model (Table

51
52 411 1). It is thus not straightforward to infer a simple relationship between genetic and surface

1
2 412 losses, since it appears that several factors (*e.g.*, level of occupancy of central Scandinavia,
3
4 413 range patchiness) bring variation to these values.

5
6 414 With regard to the predicted ranges of current gene pools (Fig. 3 D–H and S6), the South-
7
8 415 Eastern one is expected to experience the greatest range contraction, especially at the core of
9
10 416 its range (*i.e.*, the Balkans). Our predictions further indicate that the South-Western gene pool
11
12 417 is likely to become extremely fragmented in the Pyrenees and nearly disappearing from the
13
14 418 Iberian Peninsula, which is in agreement with predictions made for other European cold-
15
16 419 adapted species (Alsos *et al.* 2009). In contrast, the Alpine region is in some cases likely to
17
18 420 continue to harbor the three gene pools (red, yellow and blue) that have colonized the
19
20 421 Western, Eastern and central edges of the Alps in the last millennia, confirming what has been
21
22 422 recently proposed for other cold-adapted species from the region (Treier & Muller-Scharer
23
24 423 2011).

25
26
27
28 424

30 425 **Conclusion**

31
32 426 The novel simulation approach used in this study allowed unravelling the most likely
33
34 427 scenarios of intraspecific gene pools diffusion across time for the last 24 ky. By being
35
36 428 virtually applicable to any species, assuming that enough occurrences are available for
37
38 429 calibrating SDMs, this predictive approach thus opens exciting new research avenues. Besides
39
40 430 its obvious application for identifying the most likely phylogeographic scenario for a given
41
42 431 species, it may also be used to statistically test user-defined scenarios based on the generation
43
44 432 of appropriate null niche-based diffusion models (see Figure S7 in Supporting Information).
45
46 433 This point is appealing when using genetic markers such as AFLPs, for which coalescent-
47
48 434 based methods, such as those proposed by Carstens & Richards (2007), are not yet applicable.
49
50 435 Moreover, the method may complement coalescent approaches when using sequence-based
51
52 436 data, allowing demographic events to be directly dated, mapped and further tested. From this
53
54
55
56
57
58
59
60

1
2 437 perspective, this study is a breakthrough in interdisciplinary projects and opens new doors in
3
4 438 the understanding of the spatial and temporal evolution of species.

5
6 439

7
8 440 **Acknowledgements**

9
10 441 The authors would like to thank R. Arnoux, P. Bowler, O. Broennimann, R. Dafydd, P.
11
12 442 Duchesne, D. Gyurova, H. Hipperson, M. Howe, L. Juillerat, R. Lavigne, P. Lazarevic, N.
13
14 443 Magrou, N. Revel, M. Ronikier, N. Russell, A. Sarr, T. Suchan, Y. Triponez and N. Villard,
15
16 444 for their invaluable field and technical assistance, as well as J. R. Litman, Y.-H. E. Tsai, the
17
18 445 members of B.C. Carstens' laboratory, three anonymous reviewers and the journal editor,
19
20 446 whose comments largely improved an earlier version of this manuscript. They also thank the
21
22 447 Vital-IT High Performance Computing Center for granting access to the computer cluster, and
23
24 448 the Centre du Réseau Suisse de Floristique and the Alpine Conservatory of Gap-Charance for
25
26 449 allowing access to their databases. This work was funded by the Swiss National Science
27
28 450 Foundation (SNSF grant No. 3100A0-116778 awarded to NA). AE and NA were funded by a
29
30 451 SNSF Ambizione fellowship (PZ00P3_126624). AG, LM, WH and LP were supported by the
31
32 452 European Commission (ECOCHANGE, FP6 2006 GOCE 036866) and the SNSF
33
34 453 (BIOASSEMBLE, Nr. 31003A-125145).

35
36 454

37
38 455 **References**

39
40
41 456 Abbott R.J. & Brochmann C. (2003). History and evolution of the arctic flora: in the footsteps
42
43 457 of Eric Hulten. *Mol Ecol*, 12, 299-313.
44
45 458 Alsos I.G., Alm T., Normand S. & Brochmann C. (2009). Past and future range shifts and loss
46
47 459 of diversity in dwarf willow (*Salix herbacea* L.) inferred from genetics, fossils and
48
49 460 modelling. *Global Ecol Biogeogr*, 18, 223-239.
50
51 461 Alsos I.G., Ehrlich D., Thuiller W., Eidesen P.B., Tribsch A., Schonswetter P., Lagaye C.,
52
53 462 Taberlet P. & Brochmann C. (2012). Genetic consequences of climate change for
54
55 463 northern plants. *Proc Biol Sci B*.

- 1
2 464 Araújo M.B. & Pearson R.G. (2005). Equilibrium of species' distributions with climate.
3 465 *Ecography*, 28, 693-695.
4
5 466 Avise J.C. (2009). Phylogeography: retrospect and prospect. *J Biogeogr*, 36, 3-15.
6
7 467 Beatty G.E. & Provan J. (2011). Comparative phylogeography of two related plant species
8 468 with overlapping ranges in Europe, and the potential effect of climate change on their
9 469 intraspecific genetic diversity. *BMC Evol Biol*, 11, 29.
10
11 470 Brochmann C., Gabrielsen T.M., Nordal I., Landvik J.Y. & Elven R. (2003). Glacial survival
12 471 or *tabula rasa*? The history of North Atlantic biota revisited. *Taxon*, 52, 417-450.
13
14 472 Burnier J., Buerki S., Arrigo N., Kupfer P. & Alvarez N. (2009). Genetic structure and
15 473 evolution of Alpine polyploid complexes: *Ranunculus kuepferi* (Ranunculaceae) as a
16 474 case study. *Mol Ecol*, 18, 3730-3744.
17
18 475 Carstens B.C. & Richards C.L. (2007). Integrating coalescent and ecological niche modeling
19 476 in comparative phylogeography. *Evolution*, 61, 1439-1454.
20
21 477 Davis M.B., Shaw R.G. & Etterson J.R. (2005). Evolutionary responses to changing climate.
22 478 *Ecology*, 86, 1704-1714.
23
24 479 Després L., Lorient S. & Gaudeul M. (2002). Geographic pattern of genetic variation in the
25 480 European globeflower *Trollius europaeus* L. (Ranunculaceae) inferred from amplified
26 481 fragment length polymorphism markers. *Mol Ecol*, 11, 2337-2347.
27
28 482 Duchesne P. & Bernatchez L. (2002). AFLPOP: a computer program for simulated and real
29 483 population allocation based on AFLP data. *Mol Ecol Notes*, 3, 380-383.
30
31 484 Ehlers J. & Gibbard P.L. (2004). Quaternary glaciations: extent and chronology. In:
32 485 *Developments in Quaternary Science*. Elsevier Amsterdam; San Diego.
33
34 486 Ehrlich D., Gaudeul M., Assefa A., Koch M.A., Mummenhoff K., Nemomissa S. &
35 487 Brochmann C. (2007). Genetic consequences of Pleistocene range shifts: contrast
36 488 between the Arctic, the Alps and the East African mountains. *Mol Ecol*, 16, 2542-
37 489 2559.
38
39 490 Engler R., Randin C.F., Thuiller W., Dullinger S., Zimmermann N.E., Araujo M.B., Pearman
40 491 P.B., Le Lay G., Piedallu C., Albert C.H., Choler P., Coldea G., De Lamo X.,
41 492 Dirnbock T., Gegout J.C., Gomez-Garcia D., Grytnes J.A., Heegaard E., Hoistad F.,
42 493 Nogues-Bravo D., Normand S., Puscas M., Sebastia M.T., Stanisci A., Theurillat J.P.,
43 494 Trivedi M.R., Vittoz P. & Guisan A. (2011). 21st century climate change threatens
44 495 mountain flora unequally across Europe. *Global Change Biology*, 17, 2330-2341.
45
46 496 Etterson J.R. & Shaw R.G. (2001). Constraint to adaptive evolution in response to global
47 497 warming. *Science*, 294, 151-154.
48
49
50
51
52
53
54
55
56
57
58
59
60

- 1
2 498 Falush D., Stephens M. & Pritchard J. (2007). Inference of population structure using
3 499 multilocus genotype data: dominant markers and null alleles. *Mol Ecol Notes*, 7, 895-
4 500 908.
- 5
6 501 Fielding A.H. & Bell J.F. (1997). A review of methods for the assessment of prediction errors
7 502 in conservation presence/absence models. *Environ Conserv*, 24, 38-49.
- 8
9 503 Freedman A.H., Thomassen H.A., Buermann W. & Smith T.B. (2010). Genomic signals of
10 504 diversification along ecological gradients in a tropical lizard. *Mol Ecol*, 19, 3778-
11 505 3788.
- 12
13 506 Graham C.H., VanDerWal J., Phillips S.J., Moritz C. & Williams S.E. (2010). Dynamic
14 507 refugia and species persistence: tracking spatial shifts in habitat through time.
15 508 *Ecography*, 33, 1062-1069.
- 16
17 509 Guisan A. & Thuiller W. (2005). Predicting species distribution: offering more than simple
18 510 habitat models. *Ecol Lett*, 8, 993-1009.
- 19
20 511 Gyllencreutz R., Mangerud J., Svendsen J.-I. & Lohne Ø. (2007). DATED – a GIS-based
21 512 reconstruction and dating database of the Eurasian deglaciation. In: *Applied*
22 513 *Quaternary research in the central part of glaciated terrain* (eds. Johansson P &
23 514 Sarala P). Geological Survey of Finland.
- 24
25 515 Hartigan J.A. & Wong M.A. (1979). A K-means clustering algorithm. *Appl Stat-J Roy St C*,
26 516 28, 100-108.
- 27
28 517 Hewitt G.M. (1996). Some genetic consequences of ice ages, and their role in divergence and
29 518 speciation. *Biol J Linn Soc*, 58, 247-276.
- 30
31 519 Hewitt G.M. (1999). Post-glacial re-colonization of European biota. *Biol J Linn Soc*, 68, 87-
32 520 112.
- 33
34 521 Hugall A., Moritz C., Moussalli A. & Stanisic J. (2002). Reconciling paleodistribution models
35 522 and comparative phylogeography in the Wet Tropics rainforest land snails
36 523 *Gnarosophila bellendenkerensis*. *Proc Natl Acad Sci U S A*, 99, 6112-6117.
- 37
38 524 IPCC I.P.o.C.C. (2001). Climate Change 2001: impacts, adaptation, and vulnerability:
39 525 contribution of Working Group II to the Third Assessment Report of the IPCC. In.
40 526 Cambridge University Press Cambridge, UK.
- 41
42 527 Körner C. (2003). *Alpine plant life - Functional plant ecology of high mountain ecosystems*.
43 528 2nd edn. Springer, Heidelberg.
- 44
45 529 Labeyrie L., Cole J., Alverson K. & Stocker T. (2003). The history of climate dynamics in the
46 530 Late Quaternary. In: *Paleoclimate, global change and the future* (eds. Alverson KD,
47 531 Bradley RS & Pedersen TF). Springer Heidelberg.
- 48
49
50
51
52
53
54
55
56
57
58
59
60

- 1
2 532 Liu C., Berry P.M., Dawson T.P. & Pearson R.G. (2005). Selecting thresholds of occurrence
3 533 in the prediction of species distributions. *Ecography*, 28, 385-393.
- 4
5 534 Maiorano L., Cheddadi R., Zimmerman N.E., Pellissier L., Petitpierre B., Pottier J., Laborde
6 535 H., Hurdu B.I., Pearman P.B., Psomas A., Singarayer J.S., Broennimann O., Vittoz P.,
7 536 Dubuis A., Edwards M.E., Binney H.A. & Guisan A. (in press). Building the niche
8
9 537 through time: using 13,000 years of data to predict the effects of climate change on
10 538 tree species in Europe. *Glob Ecology & Biogeogr.*
- 11
12
13 539 Marmion M., Parviainen M., Luoto M., Heikkinen R.K. & Thuiller W. (2009). Evaluation of
14 540 consensus methods in predictive species distribution modeling. *Div Dist*, 15, 59-69.
- 15
16
17 541 Mitchell T.D., Carter T.R., Jones P.D., Hulme M. & New M. (2004). A comprehensive set of
18 542 high-resolution grids of monthly climate for Europe and the globe: the observed
19 543 record (1901-2000) and 16 scenarios (2001-2100). *Tyndall Centre Working Paper*, 55,
20 544 1-25.
- 21
22
23 545 Parducci L., Jørgensen T., Tollefsrud M.M., Elverland E., Alm T., Fontana S.L., Bennett
24 546 K.D., Haile J., Matetovici I., Suyama Y., Edwards M.E., Andersen K., Rasmussen M.,
25 547 Boessenkool S., Coissac E., Brochmann C., Taberlet P., Houmark-Nielsen M., Larsen
26 548 N.K., Orlando L., Gilbert M.T.P., Kjær K.H., Alsos I.G. & Willerslev E. (2012).
27 549 Glacial survival of boreal trees in Northern Scandinavia. *Science*, 335, 1083-1086.
- 28
29
30 550 Peakall R. & Smouse P.E. (2006). GENALEX 6: genetic analysis in Excel. Population genetic
31 551 software for teaching and research. *Mol Ecol Notes*, 6, 288-295.
- 32
33
34 552 Pritchard J.K., Stephens M. & Donnelly P. (2000). Inference of population structure using
35 553 multilocus genotype data. *Genetics*, 155, 945-959.
- 36
37
38 554 Raymo M.E. (1997). The timing of major climate terminations. *Paleoceanography*, 12, 577-
39 555 585.
- 40
41
42 556 Schmitt T. (2009). Biogeographical and evolutionary importance of the European high
43 557 mountain systems. *Front Zool*, 6, 9.
- 44
45 558 Schönswetter P., Popp M. & Brochmann C. (2006). Rare arctic-alpine plants of the European
46 559 Alps have different immigration histories: the snow bed species *Minuartia biflora* and
47 560 *Ranunculus pygmaeus*. *Mol Ecol*, 15, 709-720.
- 48
49
50 561 Singarayer J.S. & Valdes P.J. (2010). High-latitude climate sensitivity to ice-sheet forcing
51 562 over the last 120 kyr. *Quaternary Science Reviews*, 29, 43-55.
- 52
53 563 Skrede I., Eidesen P.B., Portela R.P. & Brochmann C. (2006). Refugia, differentiation and
54 564 postglacial migration in arctic-alpine Eurasia, exemplified by the mountain avens
55 565 (*Dryas octopetala* L.). *Mol Ecol*, 15, 1827-1840.
- 56
57
58
59
60

- 1
2 566 Stewart J.R., Lister A.M., Barnes I. & Dalén L. (2010). Refugia revisited: individualistic
3 567 responses of species in space and time. *Proc R Soc B*, 277, 661-671.
4
5 568 Svenning J.-C., Normand S. & Kageyama M. (2008). Glacial refugia of temperate trees in
6 569 Europe: insights from species distribution modelling. *J Ecol*, 96, 1117-1127.
7
8 570 Thuiller W., Lafourcade B., Engler R. & Araújo M.B. (2009). BIOMOD-a platform for
9 571 ensemble forecasting of species distributions. *Ecography*, 32, 369-373.
10
11 572 Treier U.A. & Muller-Scharer H. (2011). Differential effects of historical migration,
12 573 glaciations and human impact on the genetic structure and diversity of the mountain
13 574 pasture weed *Veratrum album* L. *J Biogeogr*, 38, 1776-1791.
14
15 575 Vega R., Flojgaard C., Lira-Noriega A., Nakazawa Y., Svenning J.-C. & Searle J.B. (2010).
16 576 Northern glacial refugia for the pygmy shrew *Sorex minutus* in Europe revealed by
17 577 phylogeographic analyses and species distribution modelling. *Ecography*, 33, 260-
18 578 271.
19
20 579 Vos P., Hogers R., Bleeker M., Reijans M., van de Lee T., Hornes M., Frijters A., Pot J.,
21 580 Peleman J. & Kuiper M. (1995). AFLP: a new technique for DNA fingerprinting.
22 581 *Nucleic Acids Res*, 23, 4407-4414.
23
24 582 Watts W.A., Allen J.R.M. & Huntley B. (1996). Vegetation history and palaeoclimate of the
25 583 last glacial period at Lago Grande di Monticchio, Southern Italy. *Quaternary Science*
26 584 *Reviews*, 15, 133-153.
27
28 585 Weider L.J. & Hobaek A. (2000). Phylogeography and arctic biodiversity: a review. *Ann Zool*
29 586 *Fennici*, 37, 217-231.
30
31 587 Westergaard K.B., Alsos I.G., Popp M., Engelskjon T., Flatberg K.I. & Brochmann C. (2011).
32 588 Glacial survival may matter after all: nunatak signatures in the rare European
33 589 populations of two west-arctic species. *Mol Ecol*, 20, 376-93.
34
35 590
36 591
37
38
39
40
41
42
43
44
45
46
47
48
49
50
51
52
53
54
55
56
57
58
59
60

592 Table 1 – Predicted future genetic diversities (proportion of polymorphic loci) and variation
 593 of surface occupancy for the species and each gene pool under three global circulation models
 594 and four emission scenarios. Differences to current values are shown.

Model	Average proportion of polymorphic sites	Difference to current genetic diversity (%)	Difference to current occupied surface (%)	Difference to current occupied surface for each gene pool (%)			
				Blue	Green	Yellow	Red
CGCM2-a1FI	0.0639	1.310	1.21	-100.00	58.16	-34.27	-79.75
CGCM2-a2	0.0643	1.846	13.68	-100.00	71.71	-21.41	-70.89
CGCM2-b1	0.0665	5.428	-4.01	-99.16	27.46	-19.56	-57.59
CGCM2-b2	0.0609	-3.487	5.86	-99.58	50.60	-19.71	-60.13
HAD3-a1FI	0.0649	2.847	-33.93	-100.00	23.18	-74.84	-91.14
HAD3-a2	0.0629	-0.290	-12.39	-99.79	39.25	-45.47	-80.38
HAD3-b1	0.0655	3.867	7.69	-95.79	67.00	-31.07	-60.76
HAD3-b2	0.0639	1.301	-8.35	-98.95	48.67	-46.32	-74.05
CSIRO2-a1FI	0.0475	-24.771	-55.36	-91.37	-16.83	-86.14	-70.25
CSIRO2-a2	0.0452	-28.440	-53.96	-96.21	-17.49	-81.94	-72.78
CSIRO2-b1	0.0548	-13.167	-43.53	-93.26	4.97	-81.94	-62.03
CSIRO2-b2	0.0536	-15.062	-43.02	-94.32	-0.18	-76.29	-60.13

595

596

1
2 597 **Figure Legends**
3

4 598 Fig. 1 – Genetic structure and SDM-based current projection of the species distribution model
5
6 599 of *T. europaeus* in Europe. A – Spatial genetic structure of *T. europaeus* according to the
7
8 600 STRUCTURE analysis. Proportions of the pies indicate the probability to belong to one of
9
10 601 four gene pools (green: North Scandinavia, yellow: Western and central Europe, red: South-
11
12 602 Western Europe, blue: South-Eastern Europe). B – Predicted current distribution of the
13
14 603 European globeflower. Caption: distribution range of the species, modified from Meusel *et al.*
15
16 604 (1965).
17
18
19
20

21 605
22 606 Fig. 2 – Simulated scenarios. A – Distribution and 95% quantile of fit of simulated diffusion
23
24 607 runs. The arrow indicates the two fittest simulations that correctly assigned 83.5% of the
25
26 608 genetically analyzed populations. B – The hindcasted distribution of the gene pools, as
27
28 609 defined by one of the two fittest scenarios for *T. europaeus*. Six time-points are shown. Colors
29
30 610 represent the gene pools identified by STRUCTURE. Grey regions represent unsuitable areas;
31
32 611 *i.e.*, areas falling below the ROC threshold and/or covered by ice. Dots in the first frame
33
34 612 indicate the random starting centers. Pies in the last frame indicate the observed gene pools,
35
36 613 as considered for the evaluation of fit; arrows indicate incongruence between results from the
37
38 614 diffusion model and the genetic clustering analysis.
39
40
41
42

43 615
44 616 Fig. 3 – Predicted range, pattern of future genetic diversity (proportion of polymorphic loci;
45
46 617 gradient of greys; A–C), future distribution (D–F) and gene pool occupancies (proportion of
47
48 618 occupied pixels; G) of *T. europaeus* under three global circulation models for the a1FI future
49
50 619 scenario (averaged from 2070-2010; Mitchell *et al.* 2004). A and D – CGCM2 model; B and
51
52 620 E – CSIRO2 model; C and F– HAD3 model. H – Current occupied area of each gene pool
53
54 621 (colors as in Fig. 1). The dashed line in D–F indicates the current Scandinavian range of *T.*
55
56
57
58
59
60

- 1
2
3
4
5
6
7
8
9
10
11
12
13
14
15
16
17
18
19
20
21
22
23
24
25
26
27
28
29
30
31
32
33
34
35
36
37
38
39
40
41
42
43
44
45
46
47
48
49
50
51
52
53
54
55
56
57
58
59
60
- 622 *europaeus*. Blotches of shaded areas in A–C are a mapping consequence of the coarse-grain
623 IWD interpolation algorithm.

For Review Only

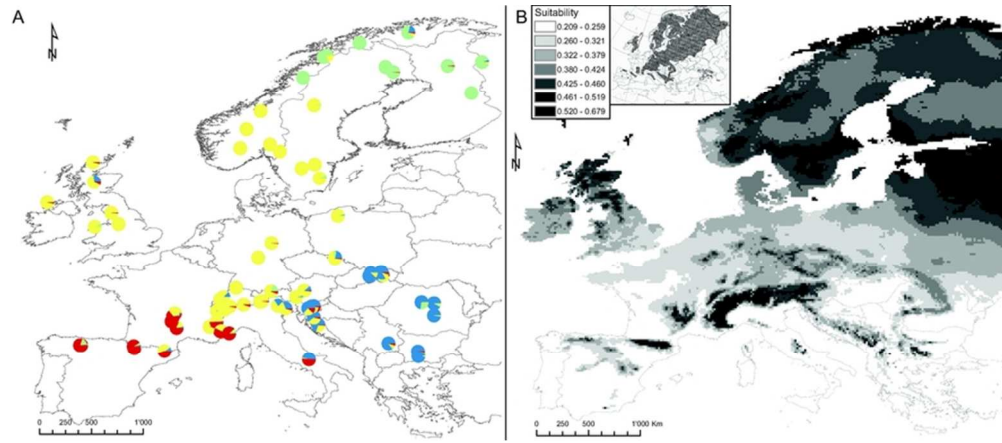


Fig. 1 – Genetic structure and SDM-based current projection of the species distribution model of *T. europaeus* in Europe. A – Spatial genetic structure of *T. europaeus* according to the STRUCTURE analysis. Proportions of the pies indicate the probability to belong to one of four gene pools (green: North Scandinavia, yellow: Western and central Europe, red: South-Western Europe, blue: South-Eastern Europe). B – Predicted current distribution of the European globeflower. Caption: distribution range of the species, modified from Meusel et al. (1965).
75x32mm (300 x 300 DPI)

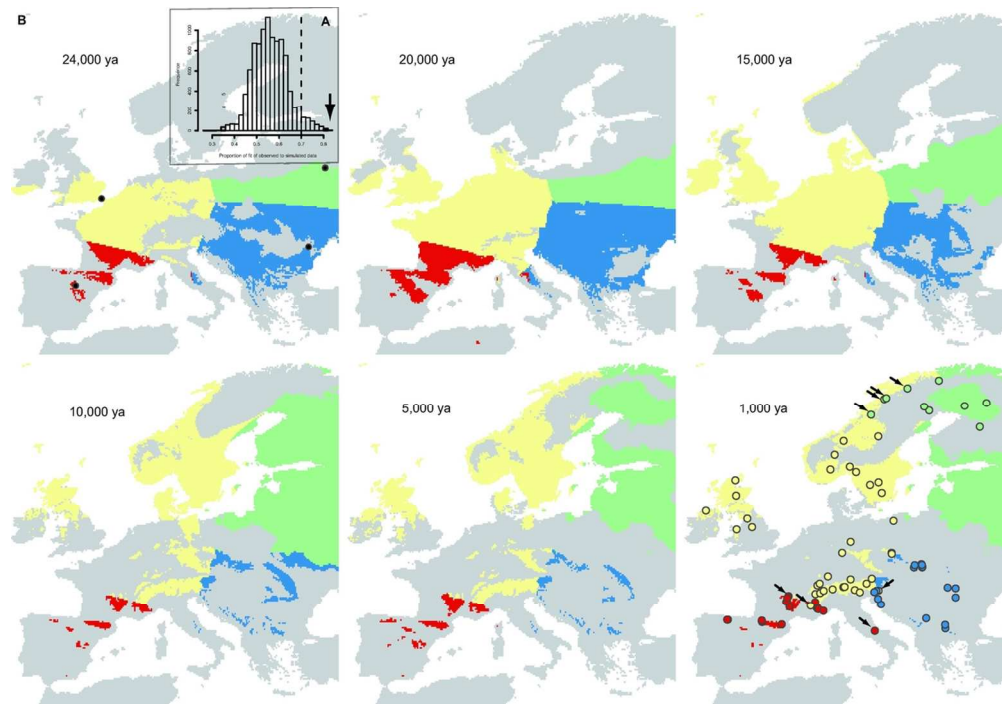


Fig. 2 – Simulated scenarios. A – Distribution and 95% quantile of fit of simulated diffusion runs. The arrow indicates the two fittest simulations that correctly assigned 83.5% of the genetically analyzed populations. B – The hindcasted distribution of the gene pools, as defined by one of the two fittest scenarios for *T. europaeus*. Six time-points are shown. Colors represent the gene pools identified by STRUCTURE. Grey regions represent unsuitable areas; i.e., areas falling below the ROC threshold and/or covered by ice. Dots in the first frame indicate the random starting centers. Pies in the last frame indicate the observed gene pools, as considered for the evaluation of fit; arrows indicate incongruence between results from the diffusion model and the genetic clustering analysis.

118x82mm (300 x 300 DPI)

1
2
3
4
5
6
7
8
9
10
11
12
13
14
15
16
17
18
19
20
21
22
23
24
25
26
27
28
29
30
31
32
33
34
35
36
37
38
39
40
41
42
43
44
45
46
47
48
49
50
51
52
53
54
55
56
57
58
59
60

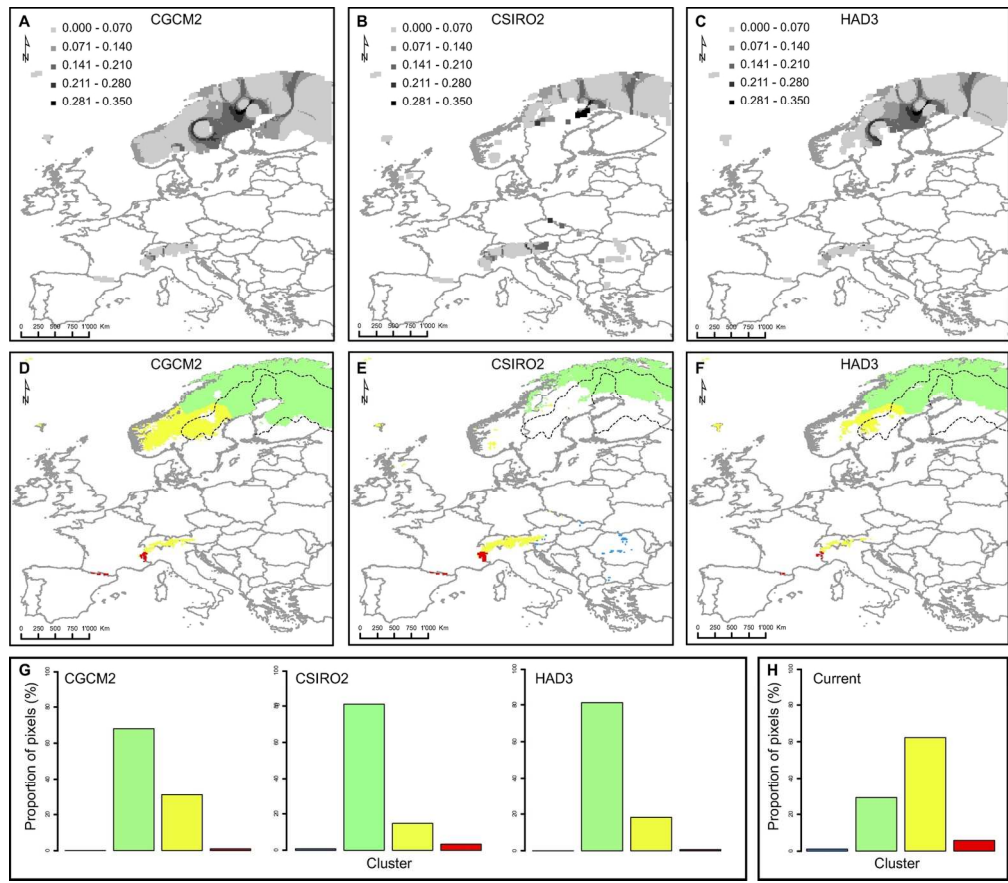


Fig. 3 – Predicted range, pattern of future genetic diversity (proportion of polymorphic loci; gradient of greys; A–C), future distribution (D–F) and gene pool occupancies (proportion of occupied pixels; G) of *T. europaeus* under three global circulation models for the a1FI future scenario (averaged from 2070–2010; Mitchell et al. 2004). A and D – CGCM2 model; B and E – CSIRO2 model; C and F– HAD3 model. H – Current occupied area of each gene pool (colors as in Fig. 1). The dashed line in D–F indicates the current Scandinavian range of *T. europaeus*. Blotches of shaded areas in A–C are a mapping consequence of the coarse-grain IWD interpolation algorithm.
150x131mm (300 x 300 DPI)